

Investigation into the linear relationship between the AE , Dst and ap indices during different magnetic and solar activity conditions

B. O. Adebésin¹

Received: 29 October 2014 / Accepted: 20 June 2015 / Published online: 14 July 2015
© Akadémiai Kiadó 2015

Abstract There are numerous geomagnetic indices used in monitoring various magnetospheric and ionospheric phenomena. Some of the most widely used indices are the ap , AE and Dst . In this work, the relationship between these three geomagnetic indices is investigated at different levels of solar and magnetic activity. 3-h average data spanning 8-years were used—high (HSA), moderate (MSA) and low solar activity (LSA) periods cover the years 1999–2001, 2004–2005, and 2006, 2009–2010 respectively. All the investigated correlation pairs recorded the highest/lowest during the LSA/HSA periods. The ap/AE correlation was found to be highest ranging within 70–78 % at any solar activity. The ap versus AE and Dst multiple correlation reached 94.0, 92.1, and 89.2 % for HSA, MSA, and LSA conditions, respectively, and 72.1, 83.3, and 80.0 % for the main phase, recovery phase and quiet conditions respectively. Moreover, higher percentage correlations were observed for the ap/AE pair at any geomagnetic conditions than for the ap/Dst and AE/Dst pairs. The ring current index Dst is observed to have a greater influence on ap during geomagnetic storm periods.

Keywords Magnetic activity · Dst index · AE index · ap index · Solar activities

1 Introduction

The continuous records available at different geomagnetic latitudes in the last century had shown that some transient variations regularly appear every day while others appear irregularly, which makes it possible to distinguish the quiet geomagnetic activities from the disturbed ones (Menvielle and Berthelier 1991). The magnetic field of the Earth, on the

✉ B. O. Adebésin
f_adebésin@yahoo.co.uk; adebésinb@gmail.com

¹ Department of Physical Sciences, College of Science and Engineering, Landmark University, P.M.B. 1001, Omu-Aran, Kwara State, Nigeria

ground, in the absence of solar-terrestrial disturbances have been found to reveal regular patterns, and is referred to as the solar quiet (Sq) variations. The Sq variations originate from electric currents flowing in the ionospheric dynamo region (80–160 km), where the electromotive force are driven by the neutral wind into the ionospheric wind dynamo system (e.g. Adebesin et al. 2013a; Richmond and Maute 2014; Yamazaki and Kosch 2014). On the other hand, geomagnetic activities originate as a consequence of the interaction between the solar wind and the magnetosphere (e.g. Kamide 1988; Adebesin and Chukwuma 2008; Adebesin et al. 2013b). Current systems that emanates from the continuous normal changes in solar radiation have been adjudged to be the main factor in the creation of Sq geomagnetic field variations (e.g. Hanslmeier 2007). This does not mean that there are no other sources. Three other sources of magnetic field variations had been reported in literatures. These are (i) variations in the Earth's heliographic latitude (Cortie 1912) (ii) the Russell–McPherron effect (Russell and McPherron 1973) and (iii) deviation in the stream of the solar wind relative to the magnetic dipole axis of the Earth (McIntosh 1959) as highlighted later by Häkkinen et al. (2003).

Various magnetic activity indices were designed to describe/measure the geomagnetic field variation observed during disturbed periods caused by the irregular current systems. According to Mayaud (1980), indices were developed in areas of enormous data availability for proper investigation and possible interrelationship description. For the purpose of this work, only the *ap*, *Dst* and the *AE* indices are considered. This is because among the various indices in use, these three appear to be the most commonly used.

The *Dst* index represents the average deviation of the geomagnetic horizontal component from its normal value reduced to the dip equator. It is obtained from four low-latitude stations, and is a measure of the strength of the ring current during the main and recovery phases of a geomagnetic storm. The *Dst* also monitors the signature of the magnetopause current during the compression phase of storms. The Auroral Electrojet (*AE*) index on the other hand, monitors the auroral electrojet (ionospheric current) during sub-storms. The *AE* index is obtained from about ten stations distributed in the northern auroral zone. The southern hemispheric distribution of observatories is far too sparse for reasonable utility in calculating the *AE* index. *AE* is calculated from the 1-min resolution data from the auroral observatories used. The average horizontal variation calculated from the five calmest magnetic days of the month is subtracted from the observed values. *AE* is then the complete range of the resulting deviations from the *AE* observatories for each minute. Visit http://geomag.usgs.gov/downloads/publications/Magnetic_Indices.pdf for information on how *AE* is obtained. See also Love and Remick (2007).

The 3-h *ap* index is derived directly from the *Kp* index, and is based only on mid-latitude observations. The *Kp* characterizes how intense the planetary magnetic activity is, especially at sub-auroral mid-latitudes. While the *Kp* is in the quasi-logarithmic scale, the *ap* is transformed into linear scale. It must be mentioned that the *Kp* index is derived from the *K* index. The *K* index gives the 3-h range of geomagnetic activity at different observatories. According to the official magnetic index webpage (<http://www.gfz-potsdam.de/en/section/earths-magnetic-field/services/kp-index/explanation/>), the *K* index (or the local disturbance level) is obtained during each 3-h time intervals by measuring the difference (∂) between the absolute maximum and minimum values for the most disturbed horizontal (*H*) magnetic field component. To achieve this, the quiet day Sq variation is first removed from the magnetogram. The maximum deviation (∂_{\max}) or the range of the *H* magnetic component is then recorded and converted to a quasi-logarithmic *K* index, by assigning a code (an integer in the range 0–9) to each 3-h interval data, according to a scale that is specific to each observatory. In this manner, the

frequency of occurrence of the various scales of disturbance is put under control. The K_p index is derived from the weighted average of the K indices at 13 sub-auroral observatories (Rostoker 1972). This compensates for the diurnal and seasonal differences between the individual observatory K values. Thereafter, the K_p indices are converted by use of a table from quasi-logarithmic scale to a nearly linear scale (ap) for easy average arithmetic activities (Le Mouël et al. 2012). The Ap index is the daily average of ap . The only advantage of ap over K_p is the change of a quasi logarithmic to a linear scale (Menvielle and Berthelier 1991). A detailed description of the derivation of these indices can be found in Mayaud (1980) and Rostoker (1972).

So far, only a few studies on the relationship of these indices have been published (e.g. Rostoker 1991; Gulyaeva 1993; Saba et al. 1994; Cade et al. 1995; Fares Saba et al. 1997; Adebesin 2008; Grimald 2013). The work of Fares Saba et al. (1997) was the first attempt to establish a relationship between the ap index and a linear combination of the AE and Dst indices. They justified the ap versus $AE + Dst$ linear relationship on the premises that currents flowing at auroral (measured with AE) and low (monitored using Dst) latitudes are supposed to uniformly affect the ap index, which is based on mid-latitude observations. They used 2 years data for their investigations: data from 1979/1974 representing the solar maximum/minimum, respectively.

This work presents a comparative linear analysis between the ap , AE and Dst indices using auto and multiple correlations, in order to study the probable relationship that exist between them quantitatively and qualitatively. The study considers different solar and magnetic activity conditions. The data used span 8 years: 3 years from the high, 2 from the moderate, and 3 from the low solar activity period. It is hoped that this work will go a long way in assisting modelling of these parameters for the different magnetic and solar activity conditions considered.

2 Methodology and treatment of data

The method used is similar to that of Fares Saba et al. (1997)—i.e. since the ap is computed at every 3-h interval, both the AE and Dst magnitudes have been averaged over the same 3-h intervals for the sake of convenience in computation. The ap , AE , and Dst relationships were considered for three solar epoch periods: the high solar activity (HSA) period spanning 1999–2001, the moderate solar activity (MSA) years 2004–2005, and the low solar activity (LSA) periods 2006, 2009–2010. More than 1 year data were employed for each of the solar activity periods so that a better statistical model for representing each solar epoch can be achieved (e.g. Adebesin et al. 2014).

All data used fall within the solar cycle 23, together with its unusually extended declining phase. A total of 8760 (i.e. 8 data/day multiplied by 365 days multiplied over 3 years) data for each index were used for both the HSA and LSA periods; whereas only about 5840 data (2 years) for the MSA period. Choice of the solar cycle 23 limited the MSA observations to 2 years. All the three indices used were obtained from the National Space Science Data Center (NSSDC) through the OMNIWEB database at <http://nssdc.gsfc.nasa.gov/omniweb>. The correlation between pairs of indices (i.e. ap versus AE , ap versus Dst , and Dst versus AE) was obtained using the Pearson correlation coefficient (R)

$$R = \frac{N \sum_i^N x_i y_i - \left(\sum_i^N x_i \right) \left(\sum_i^N y_i \right)}{\sqrt{\left(N \sum_i^N x_i^2 - \left(\sum_i^N x_i \right)^2 \right) \left(N \sum_i^N y_i^2 - \left(\sum_i^N y_i \right)^2 \right)}} \quad (1)$$

where x_i and y_i are the respective pairs of indices, N the number of datasets, and $i = 1, 2, \dots, N$. In this sense, correlation is taken as the degree of relationship between them, which seeks to determine how well a linear or non-linear equation describes the relationships between variables. To obtain the multiple correlation coefficients between the three indices (i.e. ap index on the y-axis versus $AE-Dst$ linear relationship on the x-axis) for the different solar and magnetic conditions, a MATLAB code was developed.

The correlation of the considered indices, expressed in percentages, were investigated at varying solar and geomagnetic conditions, i.e. at (i) HSA, (ii) MSA, (iii) LSA, as well as during (iv) quiet conditions, (v) storm's main phase, and (vi) storm's recovery phase.

3 Distribution of intense storms during the study period

Table 1 (after Loewe and Prolss 1997) highlights the basic classifications of geomagnetic storms based on Dst index using the 1957–1993 measurements. Great and Very intense storms are just about 5 % of the total number of storms, whereas Intense, Very intense and Great storms (with the corresponding minimum Dst values) during the study period are presented in Table 2. More intense storms were observed during the HSA years (1999–2001) with an average occurrence rate of about 10 times per year. During the MSA period (2004–2005) about 6 intense magnetic storms occurred per year on the average. However, the rate of occurrence during the LSA periods (2006, 2009–2010) was as low as 0–1 times/year.

4 Results and discussion

4.1 Annual, monthly and seasonal average values of indices

The annual, monthly, and seasonal average values of the three indices were first investigated in order to identify how they vary with interplanetary sources during the period of different magnetic and solar activities considered.

Table 1 Dst classification of geomagnetic storms using the 1957–1993 measurements (after Loewe and Prolss 1997)

Class	Number	%	Dst range (nT)
Weak	482	44	−30 to −50
Moderate	346	32	−50 to −100
Strong (i.e. intense)	206	19	−100 to −200
Severe (very-intense)	45	4	−200 to −350
Great	6	1	<−350

Table 2 List of all major intense geomagnetic storms with minimum peak *Dst* values observed during the study periods, corresponding to the high, moderate and low solar activities

Solar activity	Year	Solar flux index (F10.7) value (s.f.u)	Storm day	Nature of storm	Minimum <i>Dst</i> peak value (nT)	Storm intensity
High	1999	193	13 January	Single	-112	Intense
			18 February	Single	-123	Intense
			23 September	Single	-173	Intense
			22 October	Single	-237	Very intense
			13 November	Single	-106	Intense
	2000	203	12 February	Single	-133	Intense
			7 April	Single	-288	Very intense
			24 May	Single	-147	Intense
			16 July	Single	-301	Very intense
			11–12 August	Double	-106	Intense
					-235	Very intense
			18 September	Single	-193	Intense
			5 October	Single	-182	Intense
			14 October	Single	-107	Intense
			29 October	Single	-127	Intense
Moderate	2001	185	7 November	Single	-159	Intense
			29 November	Single	-119	Intense
			20 March	Single	-149	Intense
			31 March	Single	-387	Strong
			11 April	Single	-271	Very intense
			18 April	Single	-114	Intense
			22 April	Single	-102	Intense
			17 August	Single	-105	Intense
			26 September	Single	-102	Intense
			1–3 October	Double	-143	Intense
					-166	Intense
			21 October	Single	-187	Intense
			28 October	Single	-157	Intense
			1 November	Single	-106	Intense
			6 November	Single	-292	Very intense
			24 November	Single	-221	Very intense
Moderate	2004	106	22 January	Single	-130	Intense
			4 April	Single	-117	Intense
			25–27 June	Double	-136	Intense
					-170	Intense
			30 August	Single	-129	Intense
			7–10 November	Triple	-374	Great
					-214	Very intense
Moderate	2005	98			-263	Very intense
			18 January	Single	-103	Intense
			8 May	Single	-110	Intense

Table 2 continued

Solar activity	Year	Solar flux index (F10.7) value (s.f.u)	Storm day	Nature of storm	Minimum Dst peak value (nT)	Storm intensity
Low	2006	82	15 May	Single	-247	Very intense
			30 May	Single	-113	Intense
			13 June	Single	-106	Intense
			24 August	Single	-184	Intense
	2009	71	15 December	Single	-159	Intense
	2010	80	Nil	Nil	Nil*	Nil
			Nil	Nil	Nil**	Nil

* Minimum peak $Dst = -83$ nT and occurred on 23 July, 2009

** Minimum peak $Dst = -85$ nT and occurred on 29 May, 2010

4.1.1 Solar activities

Figure 1 depicts the monthly averages of ap , AE , and $-Dst$ for the three solar activity periods. Equal annual average magnitude was noted for the ap index for HSA and MSA periods, well above the LSA (the horizontal dashed line across the figure). Similar trend was observed for the AE index. The AE plot implies that the auroral electrojet is more intense during the MSA and HSA years, resulting in higher substorm activities. However, the average Dst was highest/lowest for the HSA/LSA periods. The highest ap and AE monthly mean values were recorded in January, occurring during the MSA years. However, Dst had its average maximum/minimum means in October/June during the HSA period. Generally, the least monthly means for all months were in LSA period. Annually, Dst recorded the maximum/minimum average values during the HSA/LSA periods, suggesting that magnetic storm is more associated with the HSA period (because of higher particle injection) than the other two solar epochs.

Seasonally (Fig. 2), the entire 8 years were considered for three seasons for the different solar epochs. These are the Equinoxes (February–April, August–October); June Solstice (May, June and July); and December Solstice (November, December and January). Each investigated index (ap , AE , Dst) is highest during the equinoxes for the HSA period. This is consistent with the result obtained by Russel and McPherron (1973), whose work had attributed higher enhancement in geomagnetic activity during the equinoctial periods. Fares Saba et al. (1997) had attributed this feature to an efficient combination of both the Earth's magnetic field and the interplanetary magnetic field. For the MSA years, the ap and Dst recorded the highest activity during December solstice, whereas June solstice recorded the highest magnitude of activity for the AE index. Equal values were recorded for ap during LSA period.

4.1.2 Magnetic activities

Three phases of a storm had been identified: the onset, main and recovery phases. The magnetic relationships between the indices were considered for the main and recovery phases and quiet condition. Data for the HSA (1999–2001) have been used for the disturbed condition, covering entirely the 21 intense ($Dst_{min} < -100$ nT) storms (see Table 2). For the quiet condition, data for an LSA year (2010) had been used. 2010 was

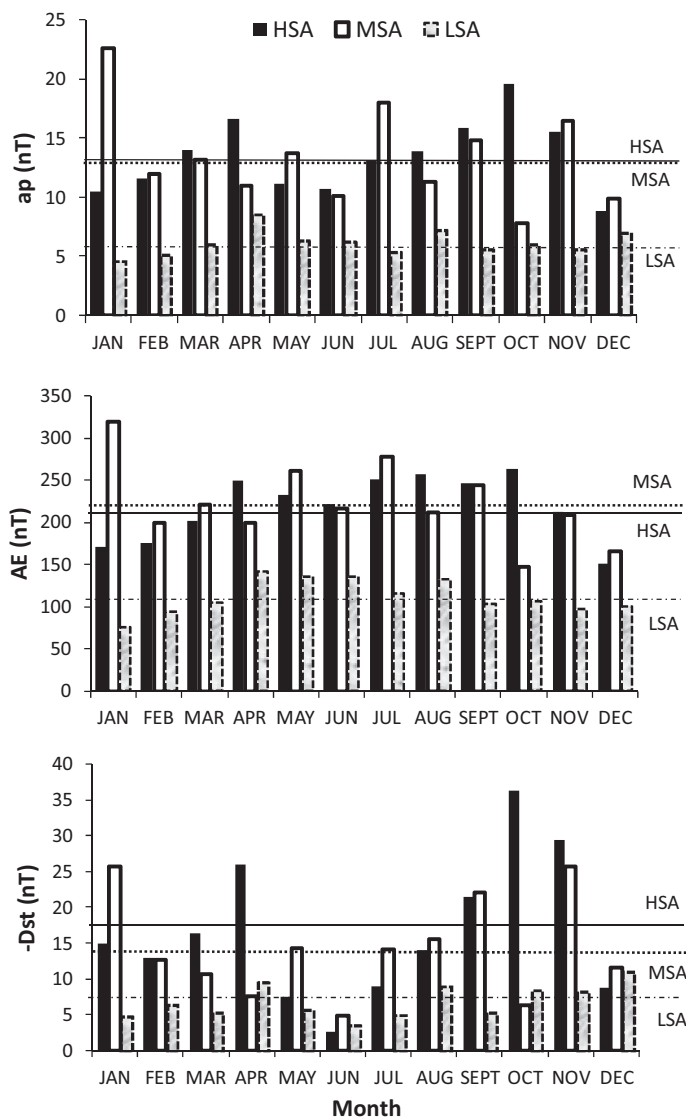


Fig. 1 Monthly mean values of ap , AE and Dst for periods of high (1999–2001), moderate (2004–2005) and low (2006, 2009–2010) solar activities. The horizontal line on each plot depicts the annual averages for each of the solar activity period. The solid thick line for HSA, dotted line for MSA, and dashed line for LSA period

characterised with no intense storm. The data were treated for extremely quiet conditions by extracting only those ap , AE and Dst data corresponding to $ap \leq 7$ nT values (e.g. Pietrella 2012; Pietrella and Perrone 2008). Nearly 81 % of all 2010 magnetic data falls within the range $ap \leq 7$ nT (see Adebesin et al. 2013a, c for the 2010 magnetic quiet characteristics). Figure 3 depicts the average ap , AE , and Dst magnitudes to all magnetic conditions. All indices recorded highest/lowest magnitude during the main phase/quiet period.

Fig. 2 Seasonal averages of ap , AE and Dst indices for HSA, MSA, and LSA periods

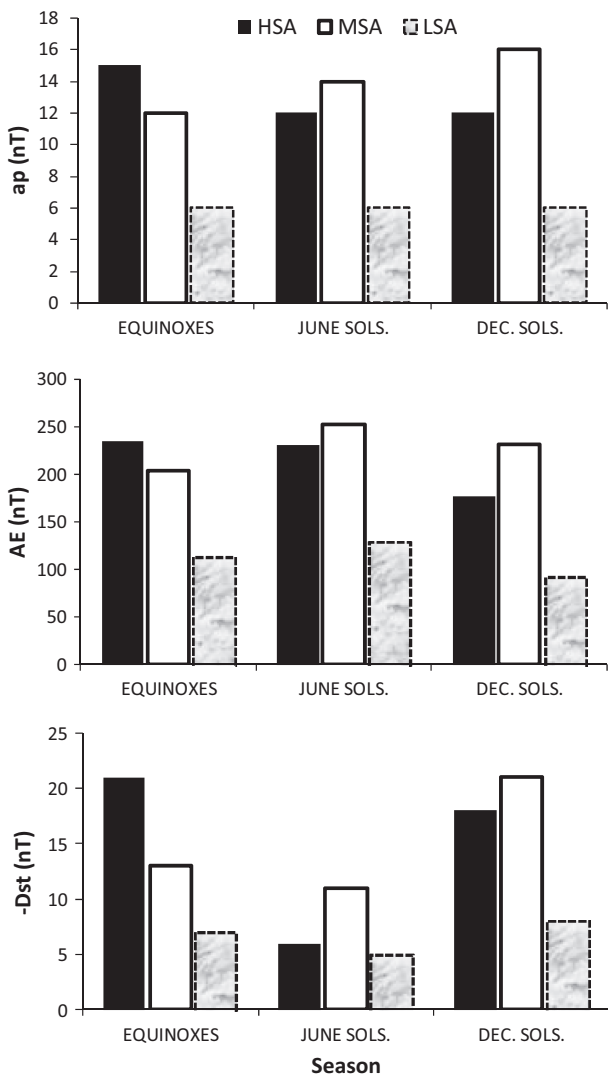
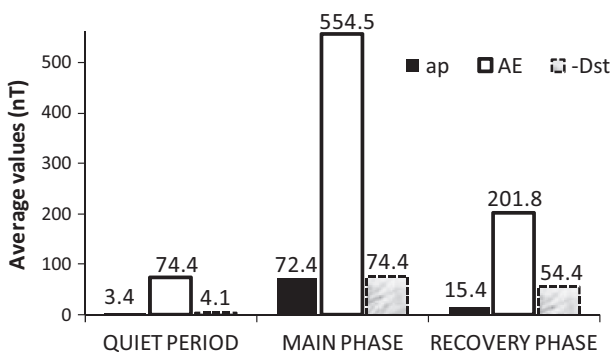


Fig. 3 Average values of ap , AE and Dst indices for the magnetic quiet period, storm's main phase and storm's recovery phase periods



4.2 Correlation analysis

4.2.1 Correlations between indices in different years and under different solar activity conditions

In Fig. 4 the annual scatter diagrams and the corresponding regression equations are shown for (top row) ap versus AE , (middle row) ap versus $-Dst$, and (bottom row) $-Dst$ versus AE . The columns are for the respective years 1999, 2000, and 2001 that constitute the HSA period. Because of space consideration, the results of the regression analyses for the MSA and LSA yearly responses are not shown. However, in order to make up for this, the respective annual correlation coefficients (R %) obtained from the regression plots for each of the years that constitute the respective HSA, MSA, and LSA periods, together with their averages has been presented in Table 3. The highest correlation was found for the ap/AE pair throughout all the years presented in the Table, irrespective of the solar activity period the year represents. This is generally followed by the $ap/-Dst$ pair, while the $-Dst/AE$ correlation was typically the weakest. The only exceptions to the above statement are the years 2005 and 2010, when the correlation of the $ap/-Dst$ pair was slightly lower than that of the $-Dst/AE$ pair. Taking all years, the correlation strength of the ap/AE , $ap/-Dst$ and $-Dst/AE$ pairs ranged between 66–78, 60–69, and 47–64 % respectively.

The results of the regression analyses for the HSA, MSA and LSA periods are summarized in the bar graph of Fig. 5. It was found, that the correlation between ap/AE , $ap/-Dst$ and $AE/-Dst$ pairs was the highest during the LSA period, while the lowest correlation was observed in HSA years. The high correlation values obtained for the LSA above the HSA are attributed to intermittent streams which possibly make the storm-time disturbance steadier along the LSA years and not outburst as in the HSA years.

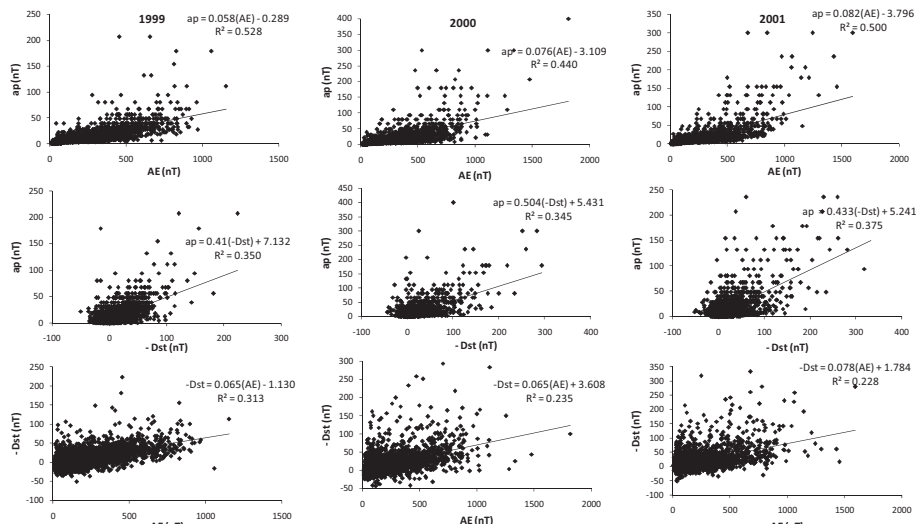
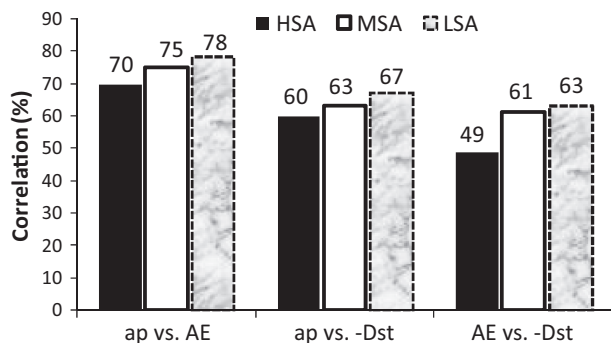


Fig. 4 Typical representation of scatter diagrams of annual 3-h mean values to determine the regression (R^2) plot for (i) ap versus AE (ii) ap versus $-Dst$, and (iii) $-Dst$ versus AE . The plot is for the respective years 1999, 2000 and 2001 that constitutes the HSA period

Table 3 Annual correlation (R %) between the three indices (in pairs) for the years considered

Solar activity	Year	Correlation		
		<i>ap</i> versus <i>AE</i> (%)	<i>ap</i> versus <i>-Dst</i> (%)	<i>-Dst</i> versus <i>AE</i> (%)
HSA	1999	73	59	56
	2000	66	59	48
	2001	71	61	48
	HSA average	70	60	49
MSA	2004	73	71	62
	2005	78	59	62
	2006	78	69	59
	MSA average	75	63	61
LSA	2009	76	65	47
	2010	77	61	64
	LSA average	78	67	63

Fig. 5 Solar activity correlation for (i) *ap* versus *AE* (ii) *ap* versus *-Dst*, and (iii) *AE* versus *-Dst*. The correlation percentage for each case is shown on top of each plot

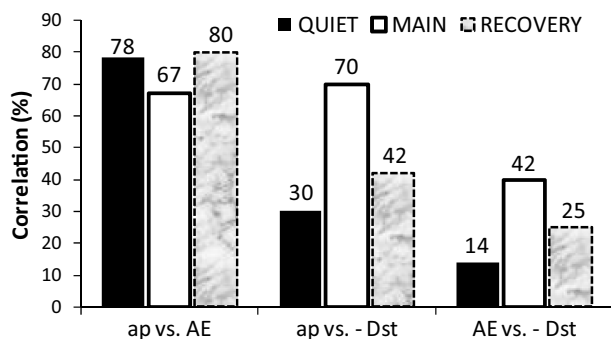


4.2.2 Correlations between indices during periods of different geomagnetic activity

Figure 6 presents the correlation between the different indices considered under different geomagnetic conditions. Generally, the highest correlations were observed for the *ap/AE* pair under quiet geomagnetic conditions, as well as during the recovery phase of storms. Regarding the magnetic activity, the highest correlation (80 %) for the *ap/AE* pair was detected during the storm's recovery phase, while the lowest (67 %) during the storm's main phase. Fares Saba et al. (1997) had observed similar characteristic. The fact that the lowest *ap/AE* correlation (67 %) was obtained during the main storm phases may have narrowed down to the effect of the intense ring current activity over the *ap* index and the rapid fluctuation of the *AE* when the auroral electrojets vary during this phase.

The *ap/Dst* and *AE/Dst* correlations followed similar pattern to each other—the highest correlation was observed during the main phase (70 and 42 %), it was followed by the recovery phase (42 and 25 %), and the lowest correlation was found under quiet conditions (30 and 14 %). In comparison, while for the *ap/AE* pair the lowest correlation was recorded during the main phase, for the cases of *ap/Dst* and *AE/Dst* pairs the highest correlations were reached in this phase.

Fig. 6 Same as in Fig. 5, but for different magnetic activity period



4.3 Multiple correlation treatment

The *ap* index has been found to account for the planetary geomagnetic activity. This is because it gains support from both the auroral electrojet (measured using *AE* index) and the ring current, using *Dst* as indicator (e.g. Rostoker 1972). Further, while the *AE* is measured at high latitudes, the *Dst* at low latitudes, the *ap* is measured at mid-latitudes (Rostoker 1972; Mayaud 1980; Amory-Mazaudier 2009). Therefore, modelling the *ap* index by a linear combination of the *AE* and *Dst* indices over a wide range of input data, under different geomagnetic and solar activity conditions could be useful for general space weather studies and others. It is also believed that ascertaining the relationship between different geomagnetic indices can characterise the activities of the whole magnetosphere and the surrounding interplanetary medium (e.g. Mayaud 1980). Multiple correlation analysis was realized by fitting the data with a linear equation of the form:

$$ap = a + b(AE) + c(-Dst) \quad (2)$$

where ‘*a*’, ‘*b*’, and ‘*c*’ are the linear fit coefficients. Correlation between *ap* and the resulted linear combination of *AE* and *Dst* was also computed. Fares Saba et al. (1997) were the first to carry out this kind of investigation.

Table 4 highlights the values of the respective multiple percentage correlation coefficients, linear fit coefficients (with associated errors and 95 % CI values) during different solar activity periods. The errors were obtained alongside other constants from the MATLAB programme that was developed using codes. The respective multiple correlation coefficients of ‘*ap* versus *AE* and *Dst*’ are 94.0, 92.1, and 89.2 % for HSA, MSA, and LSA conditions. A comparison of the values with correlation pairs of Fig. 5 showed that the former (i.e. multiple pair) are evidently higher for each investigated solar activity period (HSA, MSA, LSA). Further, the linear fit coefficient ‘*a*’ is small, suggesting that *ap* is well explained by the independent variables (e.g. Rostoker 1972; Fares Saba et al. 1997). Both ‘*b*’ and ‘*c*’ are not simply the weight of the considered variable, but also a kind of scale factor.

Values of the respective correlation and linear fit coefficients with other parameters for varying geomagnetic activity conditions are shown in Table 5. Data for all of the 21 intense ($Dst_{min} < -100$ nT) storms spanning HSA period (1999–2001) have been used to characterise both the main and recovery phases; while the LSA year 2010 data for which $ap \leq 7$ nT has been used to characterise the quiet condition (see Table 2). Higher multiple correlation coefficients are observed during both the quiet period (80.0 %) and the

Table 4 Multiple correlation (i.e. ap versus AE versus Dst) for different solar activity periods, with corresponding linear fit coefficients, errors (inside brackets) and CI

Solar activity period	Correlation coefficient (%)	a	CI for a*	b ($\times 10^{-2}$)	CI for b ($\times 10^{-2}$)*	c ($\times 10^{-2}$)	CI for c ($\times 10^{-2}$)*
High	94.0	1.41 (0.01)	−1.20–4.02	3.82 (0.00)	2.56–5.08	22.34 (0.28)	17.57–27.12
Moderate	92.1	−2.68 (0.25)	−7.11–1.74	5.60 (0.01)	3.27–7.94	25.08 (0.08)	9.32–40.83
Low	89.2	0.23 (0.08)	−1.54–1.99	3.62 (0.62)	2.21–5.03	26.97 (0.01)	14.43–39.52

* CI is at 95 % level

Numbers inside brackets are the respective errors associated with each set of observation

recovery phase (83.3 %), well above the observation during storm's main phase (72.1 %). Here, the linear fit coefficient 'a' has increased especially for the main and recovery phases of the ionospheric and magnetospheric perturbations over the values observed for varying solar activities (in Table 4). This is because the planetary magnetic activity index ap during both the main and recovery phases are higher. Further, Fig. 6 ap/AE versus Table 5 reveals that the addition of Dst to the ap/AE correlation increased the correlation strengths slightly, suggesting that Dst has greater influence on ap during episodes of high ring current activity.

5 Comparison with previous result

Most ionospheric/magnetospheric disturbances are observed in the low and high latitude regions. Therefore both the AE and Dst magnetic parameters are useful in identifying magnetic activities. The ap is also useful as it spreads around the AE (in high latitude) and Dst (in low latitude). The ap numerical values are related to the magnitude of the disturbance at a standard mid-latitude station (Rostoker 1972). As earlier mentioned, only Fares Saba et al. (1997) have presented multiple correlation analysis between the ap , AE , and Dst indices in a single model equation for different kinds of activities (except otherwise argued). Comparison in terms of both the correlation coefficient (Table 6) and the linear fit coefficients (Table VII) were therefore made with the present work. Fares Saba et al. (1997) had made use of 3-h average data of 1974 (representing LSA) and 1979 (for HSA). The present study data spans 1999–2001 (HSA) and 2006, 2009 and 2010 (LSA). The results for both the MSA and quiet magnetic conditions observed in this work are not indicated on both tables (Tables 6, 7) as there is no result available for comparison.

The respective correlation coefficients depicted in Table 6 revealed a good agreement between the two results for all conditions considered. On the average both results agreed by as much as 98 % (Fig. 7). Little difference in magnitudes was observed between the two works for all conditions considered on the Table. Table 7 compares the respective linear fit coefficients for the multiple correlation procedures from both results, and the following characteristics were observed in their absolute values: (i) linear fit coefficient 'c' is almost equal during both the LSA and HSA periods for both results (ii) 'c' is lower during the recovery phase than the main phase for both set of results, though with larger difference in the present study (iii) during the magnetic activity period, 'b' is stronger during the main

Table 5 Multiple correlation for different magnetic activity periods with corresponding linear fit coefficients, errors (inside brackets) and CI

Magnetic activity period	Correlation coefficient (%)	a	CI for a*	b ($\times 10^{-2}$)	CI for b ($\times 10^{-2}$)*	c ($\times 10^{-2}$)	CI for c ($\times 10^{-2}$)*
Quiet condition	80.0	1.27 (1.74)	0.64–1.89	2.70 (2.40)	1.89–3.52	3.30 (1.53)	-1.42–8.02
Main phase	72.1	-28.64 (0.91)	-60.81–3.52	10.89 (1.56)	4.80–16.98	54.45 (12.66)	31.73–77.17
Recovery phase	83.3	-5.98 (0.61)	-15.03–3.07	6.55 (0.10)	4.28–8.83	15.05 (5.62)	-0.08–30.18

* CI is at 95 % level

Numbers inside brackets are the respective errors associated with each set of observation

phase than the recovery phase in the present work, whereas the reverse is the case for the former result, and (iv) ‘*a*’ is larger in absolute sense during the main phase than the recovery phase for both results. On the average, observations from both results are consistent.

The larger difference obtained for the linear fit coefficient ‘*c*’ between the main and recovery phases ($54.5 - 15.1 = 39.4$) in the present work as compared with the ‘*c*’ = 24.0 *gap* for the earlier result may have come up as a result of the nature and magnitude of the intensity of storms considered in each work. Fares Saba et al. (1997) had considered 7 intense and 11 moderate storms from 1979 to characterise their magnetic storm activity, whereas the present work had considered all 21 intense storms from 1999 to 2001. If to go by this, it is expected that the recovery phase observations in the present study will last longer (for *Dst*) for intense storms than for some moderate storms considered by the earlier work. Hence the reason for the wider *gap* in ‘*c*’. Additionally, both results exhibited the highest correlation values for the *ap/AE* pair compared to other pairs of indices (*ap/Dst* and *AE/Dst*) for the different solar activity (HSA, MSA, LSA) conditions (see Figs. 5, 8).

6 Summary and conclusion

The correlations between the magnetic indices *ap*, *AE* and *Dst*, both in pairs and in multiple correlations were investigated under different magnetic and solar activity conditions. This include HSA (1999–2001), MSA (2004–2005) and LSA (2006, 2009–2010) periods; as well as the periods of main and recovery phases of geomagnetic activity and magnetic quiet condition.

For the solar activity condition, the pairs of *ap/AE*, *ap/Dst* and *AE/Dst* reached the highest correlation during the LSA period. The lowest correlation was recorded in HSA years. The higher correlations observed during the LSA period compared to the HSA

Table 6 Comparison of multiple correlation coefficient results for different magnetic and solar activity conditions

Activity	Correlation coefficient (%)			
	HSA/year	LSA/year	Main phase	Recovery phase
Fares Saba et al. (1997)	94.4	94.1	79.3	87.7
Present work	94.0	89.2	72.1	83.3

Table 7 Comparison of multiple linear fit coefficients results for different magnetic and solar activity conditions

Linear fit coefficient	a		b ($\times 10^{-2}$)		c ($\times 10^{-2}$)	
	Fares Saba et al. (1997)	Present work	Fares Saba et al. (1997)	Present work	Fares Saba et al. (1997)	Present work
HSA/year	−2.9	1.4	6.1	3.8	23.1	22.3
LSA/year	3.3	0.2	4.6	3.6	23.6	26.9
Main phase	−15.8	−28.6	4.5	10.9	66.0	54.5
Recovery phase	−13.7	−6.0	6.6	6.6	42.0	15.1

Fig. 7 Scatter plot between the correlation results obtained by Fares Saba et al. (1997) and the present work

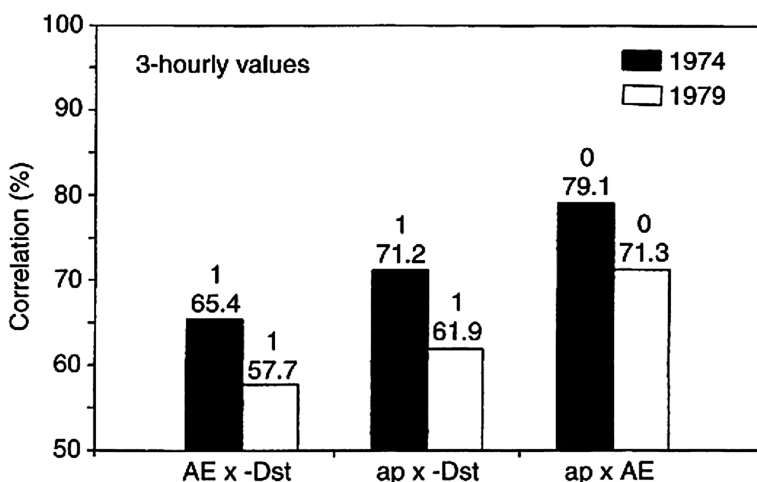
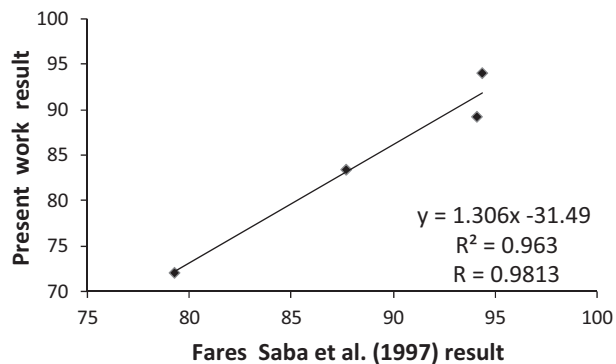


Fig. 8 Solar activity correlation for (i) AE versus $-Dst$ (ii) ap versus $-Dst$, and (iii) ap versus AE . The correlation percentage for each case and time lag is shown on top of each column (after Fares Saba et al. 1997)

period are attributed to recurring high speed streams which possibly make the geomagnetic perturbation more stable during years of LSA, and not outburst as in the HSA years (e.g. Fares Saba et al. 1997). In accordance with previous results, the ap/AE correlation was found to be the highest (70–78 %) of all pairs considered at any solar activity. The respective multiple correlation coefficients of ' ap versus AE and Dst ' are 94.0, 92.1, and 89.2 % for HSA, MSA, and LSA conditions, and are higher than the corresponding percentages recorded for the set of pair observations.

For the magnetic correlation between pairs of respective indices, higher percentage correlations were observed for the ap/AE relationship at any geomagnetic conditions. Regarding the magnetic activity, the highest correlation (80 %) for the ap/AE pair was detected during the storm's recovery phase, with the lowest (67 %) during the storm's main phase. The ap/Dst and AE/Dst correlations follow similar pattern to each other—the highest correlation during the main phase (70 and 42 %), followed by the recovery phase

(42 and 25 %), and the lowest under quiet conditions (30 and 14 %). Higher multiple correlation coefficients are observed during both the quiet period (80.0 %) and the recovery phase (83.3 %), well above the observation during storm's main phase (72.1 %).

The investigated indices, ap , AE and Dst , have highest average values during the equinoxes for the HSA period. Further, index predictability is seen as an important tool in space weather applications and a host of many other fields. As a result, model equations with linear fit correlation coefficients were developed for the different solar and magnetic activity conditions. These are:

$$\text{High solar activity : } ap = 1.41 + 3.82 \times 10^{-2}(AE) + 22.34 \times 10^{-2}(-Dst) \quad (3)$$

$$\text{Moderate solar activity : } ap = -2.68 + 5.60 \times 10^{-2}(AE) + 25.08 \times 10^{-2}(-Dst) \quad (4)$$

$$\text{Low solar activity : } ap = 0.23 + 3.62 \times 10^{-2}(AE) + 26.97 \times 10^{-2}(-Dst) \quad (5)$$

$$\text{Storm main phase : } ap = -28.64 + 10.89 \times 10^{-2}(AE) + 54.45 \times 10^{-2}(-Dst) \quad (6)$$

$$\text{Storm recovery phase : } ap = -5.98 + 6.55 \times 10^{-2}(AE) + 15.05 \times 10^{-2}(-Dst) \quad (7)$$

$$\text{Magnetic quiet condition : } ap = 1.27 + 2.70 \times 10^{-2}(AE) + 3.30 \times 10^{-2}(-Dst) \quad (8)$$

Lastly, the results of the present work are consistent with previous results. The ring current index Dst is observed to have a greater influence on ap during geomagnetic storm periods (Eq. 6). It is hoped that the model Eqs. (3)–(8) would be of great benefit as estimates in filling gaps that may be due to human/machine error in the data repositories of these indices for different magnetic and solar activity conditions, especially during the solar cycle 23. Further, establishing the relationship between different geomagnetic indices can characterise the activities of the entire magnetosphere and that of its interplanetary medium.

Acknowledgments The author is grateful to the National Space Science Data Center (NSSDC) through the OMNIWEB database (<http://nssdc.gsfc.nasa.gov/omniweb>) for the hourly data of the magnetic indices used. I will like to thank the three reviewers for their positive criticism and suggestions, which had improved the quality and structure of the paper.

References

- Adebesin BO (2008) Roles of Interplanetary and Geomagnetic parameters in ‘intense’ and ‘very intense’ magnetic storms generation and their geoeffectiveness. *Acta Geod et Geophys Hung* 43(4):383–408. doi:10.1556/AGeod.43.2008.4.2
- Adebesin BO, Chukwuma VU (2008) On the variation between Dst and IMF Bz during ‘intense’ and ‘very intense’ geomagnetic storms. *Acta Geod et Geophys Hung*, 43(1):1–15. doi:10.1556/AGeod.43.2008.1.1. ISSN 1217-8977
- Adebesin BO, Adeniyi JO, Adimula IA, Reinisch BW, Yumoto K (2013a) F2 layer characteristics and electrojet strength over an equatorial station. *Adv Space Res* 52(5):791–800. doi:10.1016/j.asr.2013.05.025
- Adebesin BO, Ikubanni SO, Adebiyi JS, Joshua BW (2013b) Multi-station observation of ionospheric magnetic disturbance of March 9 2012 and comparison with IRI model. *Adv Space Res* 52(4):604–613. doi:10.1016/j.asr.2013.05.002
- Adebesin BO, Adeniyi JO, Adimula IA, Reinisch BW (2013c) Equatorial vertical plasma drift velocities and electron densities inferred from ground-based ionosonde measurements during low solar activity. *J Atmos Solar Terr Phys* 97:58–64. doi:10.1016/j.jastp.2013.02.010

- Adebesin BO, Adekoya BJ, Ikubanni SO, Adebiyi SJ, Adebesin OA, Joshua BW, Olonade KO (2014) Ionospheric foF2 morphology and response of F2 layer height over Jicamarca during different solar epochs and comparison with IRI-2012 model. *J Earth Syst Sci* 123(4):751–765. doi:10.1007/s12040-014-0435-y
- Amory-Mazaudier C (2009) Electric current systems in the earth's environment. *Niger J Space Res* 8:178–255
- Cade WB, Sojka JJ, Zhu L (1995) A correlative comparison of the ring current and auroral electrojets using geomagnetic indices. *J Geophys Res* 100:97–105
- Cortie AL (1912) Sunspots and terrestrial magnetic phenomena, 1898–1911. *Mon Not R Astron Soc* 73:52–60
- Fares Saba MM, Gonzalez WD, Clua de Gonzalez AL (1997) Relationships between the *AE*, *ap* and *Dst* indices near solar minimum (1974) and at solar maximum (1979). *Ann Geophys* 15:1265–1270
- Grimald SR (2013) A comparative study of *Kp*, *Ap*, *Km*, *Am*, *Dst* and *AE* index. *Geophys Res Abstr* 15:5316
- Gulyaeva TL (1993) Indices of geomagnetic variations and ionospheric disturbances. *Adv Space Res* 13(3):21–31. doi:10.1016/0273-1177(93)90243-5
- Häkkinen LVT, Pulkkinen TI, Pirjola RJ, Nevanlinna H, Tanskanen EI, Turner NE (2003) Seasonal and diurnal variation of geomagnetic activity: revised *Dst* versus external drivers. *J Geophys Res A* 108(A2):1060. doi:10.1029/2002JA009428
- Hanslmeier A (2007) The Sun and space weather. Astrophysics and space science library, 2nd edn. Springer, Netherland, p 191. doi:10.1007/978-1-4020-5604-8
- Kamide Y (1988) Electrodynamical processes in the Earth's ionosphere and magnetosphere. Kyoto Sangyo University Press, Kyoto
- Le Mouël J-L, Blanter E, Shnirman M, Courtillot V (2012) On secular changes of correlation between geomagnetic indices and variations in solar activity. *J Geophys Res* 117:A09103. doi:10.1029/2012JA017643
- Loewe CA, Prolss GW (1997) Classification and mean behavior of magnetic storms. *J Geophys Res* 102:14209
- Love JJ, Remick KJ (2007) Magnetic indices. In: Encyclopedia of geomagnetism and paleomagnetism. Springer, Dordrecht, pp 509–512. http://geomag.usgs.gov/downloads/publications/Magnetic_Indices.pdf
- Mayaud PN (1980) Derivation, meaning and use of geomagnetic indices. Geophysical monograph 22. American Geophysical Union, Washington, DC
- McIntosh D (1959) On annual variation of magnetic disturbance. *R Soc Lond* 251:525–552
- Menvielle M, Berthelier A (1991) K-derived planetary indices: description and availability. *Rev Geophys* 29(3):415–432
- Pietrella M (2012) A short-term ionospheric forecasting empirical regional model (IFERM) to predict the critical frequency of the F2 layer during moderate, disturbed, and very disturbed geomagnetic conditions over the European area. *Ann Geophys* 30:343–355. doi:10.5194/angeo-30-343-2012
- Pietrella M, Perrone L (2008) A local ionospheric model for forecasting the critical frequency of the F2 layer during disturbed geomagnetic and ionospheric conditions. *Ann Geophys* 26:323–334
- Richmond AD, Maute A (2014) Ionospheric electrodynamics modeling. In: Huba J, Schunk R, Khazanov G (eds) Modeling the ionosphere-thermosphere system. Wiley, Chichester, pp 57–71. doi:10.1002/9781118704417.ch6
- Rostoker G (1972) Geomagnetic indices. *Rev Geophys Space Phys* 10:157
- Rostoker G (1991) A quantitative relationship between *AE* and *Kp*. *J Geophys Res* 96:5853–5857
- Russell CT, McPherron RL (1973) Semi-annual variation of geomagnetic activity. *J Geophys Res* 78:92–108
- Saba M, Gonzalez WD, Gonzalez ALC (1994) Relationship between the *Dst*, *ap* and *AE* indices. *Adv Space Res* 14:435–438
- Yamazaki Y, Kosch MJ (2014) Geomagnetic lunar and solar daily variations during the last 100 years. *J Geophys Res Space Phys* 119:6732–6744. doi:10.1002/2014JA020203